Paper 33-2 has been designated as a Distinguished Student Paper at Display Week 2025. The full-length version of this paper appears in a Special Section of the *Journal of the Society for Information Display (JSID)* devoted to Display Week 2025 Distinguished Papers. This Special Section will be freely accessible until December 31, 2025 via:

https://sid.onlinelibrary.wiley.com/doi/full/10.1002/jsid.2063

Authors that wish to refer to this work are advised to cite the full-length version by referring to its DOI:

https://doi.org/10.1002/jsid.2063

High-Efficiency Low-Crosstalk Red AlGaInP MicroLEDs with Continuous Multiple Quantum Wells for Low-Power AR Glasses

Yizhou Qian[1], Seok-Lyul Lee[2], and Shin-Tson Wu[1]
[1]College of Optics and Photonics, University of Central Florida, Orlando FL
[2]AU Optronics Corp., Hsinchu Science Park, Hsinchu 300, Taiwan

Abstract
By redirecting the reflected wave and implementing meta-atoms in the device structure, the light extraction efficiency of continuous multiple-quantum-well red AlGaInP microLED is improved by ~30% while suppressing the crosstalk between adjacent pixels. By implementing carbon black matrix, the crosstalk is reduced by 5 times while maintaining a high efficiency. These high-efficiency red microLEDs help reduce the power consumption and improve image quality of emerging full-color AR eyeglasses.

Author Keywords
MicroLED; Microdisplay; AR and VR displays

1. Introduction
MicroLED is emerging as a strong contender for augmented reality (AR) light engines due to its high peak luminance, long lifetime, and excellent image quality [1]. However, the efficiency of microLEDs decreases dramatically as the pixel size shrinks, primarily because of the sidewall defects during dry etching [2]. This performance degradation results in a compromised external quantum efficiency (EQE), especially for red AlGaInP micro-LEDs, which in turn leads to an increased power consumption in full-color AR eyeglasses. Although applying surface passivation and wet etching can alleviate this issue, these methods often reduce the emission area and cause nonuniformity. At 2024 SID Display Week, JBD introduced a continuous multiple quantum well (CMQW) red AlGaInP microLED [3]. Unlike the pixelated chips, the active region of the CMQW microLED extends across the entire panel, avoiding etch damage to the active layers. Such a new structure boosts efficiency by 3.5×.

Despite these advancements, CMQW microLEDs still face significant challenges. First, the low light extraction efficiency (LEE) in red AlGaInP LEDs remains to be overcome. The large refractive index mismatch between AlGaInP and the dielectric passivation layer or indium tin oxide (ITO) causes the emitted light to be trapped within the structure, eventually being absorbed by metal contacts or the absorptive AlGaInP material. Second, due to the limited etching accuracy, a minimum of 300nm thick AlGaInP, including the active region, must remain connected between adjacent pixels. This connection leads to electrical and optical crosstalk: current diffusion can induce an unwanted excitation in neighboring pixels, and the CMQW structure can act as a waveguide, causing light leakage into adjacent pixels.

In this paper, we simulate and evaluate both the electrical and optical performance of CMQW red microLEDs. Our results agree well with the measured data reported by JBD, validating our simulation approach. We analyze the loss mechanisms within the CMQW structure and propose practical solutions compatible with current fabrication capabilities. By redirecting reflected waves and implementing meta-atoms, we optimize the structure, increasing the effective LEE from 6.4% to 8.28%. Crosstalk between adjacent pixels is also reduced from 19.5% to 15%. By implementing carbon black matrix (BM), the crosstalk dramatically reduces from 19.5% to 3.8%, corresponding to a 5× improvement, while the effective LEE still remains at 6.87%, which is even higher than the unoptimized device. This significant reduction in crosstalk enhances overall image quality and minimizes image blur. Further enhancements, such as better control of current diffusion and advanced optimization of meta-atoms, are promising avenues for achieving an even higher LEE and lower crosstalk.

2. Electrical performance of CMQW structure
Silvaco TCAD (Silvaco Inc., Santa Clara) is employed to perform 2D CMQW microLED simulation. As shown in Fig. 1(a), three adjacent pixels are simulated to calculate the electrical performance and crosstalk of the structure. As reported by JBD, the total thickness of CMQW microLED is below 1μm. To achieve such a thin film, the AlGaInP microLED needs to be polished. In our simulation, the P-type AlGaInP layer is Mg-doped and N-type AlGaInP layer is Si-doped. Both doping is 10^{19} cm^{-3}. In the active region, the bandgap of AlGaInP is dependent on the Al, Ga, and In compositions.

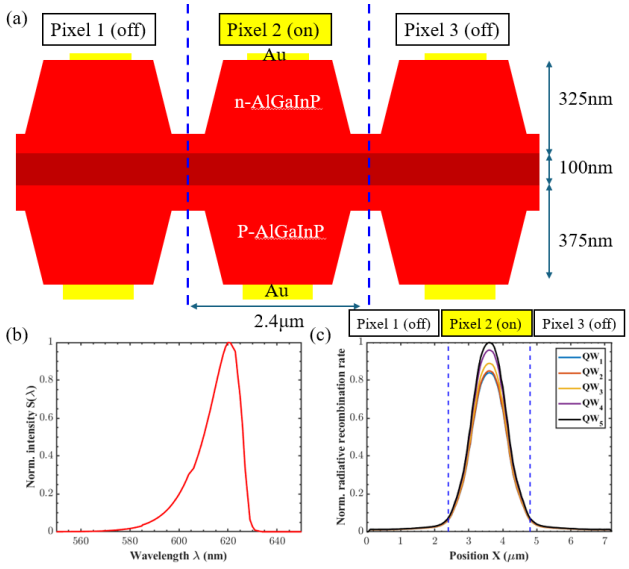

Figure 1. (a) CMQW electrical model in Silvaco TCAD. (b) Simulated normalized emission spectra. (c) Simulated normalized radiative reconbination rate.

ISSN 0097-996X/25/5601-0429-$1.00 © 2025

To obtain a 620nm peak wavelength, we apply $Al_{0.15}Ga_{0.3}In_{0.55}P$ in the MQW and the full-width-at-half-maximum is only 18nm as shown in Fig. 1(b). To increase the quantum confinement, we applied $(Al_{0.5}Ga_{0.5})_{0.52}In_{0.48}P$ as quantum barrier whose energy gap is approximately 2.2 eV. Figure 1(c) indicates the normalized radiative recombination rate in the active region when the current density is 30A/cm^2 and the applied voltage is 2.02V. Although the electrical crosstalk to adjacent pixels is only 7%, the excitation of dipoles close to adjacent pixels still induces some optical crosstalk.

3. Optical performance of CMQW structure

Red CMQW AlGaInP microLED model is built in the finite-difference time-domain (FDTD, Ansys) software as shown in Fig. 2(a). A total of three pixels are simulated to calculate the optical crosstalk and the total simulation region width (W) is 9μm. The boundary condition is steep angle perfect matched layer. On top of each pixel, photonic crystal with 140nm diameter and 200nm periodicity is laminated on top surface of the ITO electrode. The top Au electrode is thinned to 9nm to ensure a high transparency [4]. Si_3N_4 dielectric passivation layer is applied on both side of the CMQW microLED to avoid conductivity. Between adjacent pixels, trapezoidal bottom metallic and inverted trapezoidal top dielectric pixel definition pillars are applied to reduce optical crosstalk. The dispersion of all the materials is considered [5]. The whole structure is immersed in polyimide whose refractive index is 1.5 and boundary condition is steep-angle perfect matched layer. A power monitor is placed on top of the structure to calculate the emission power and optical crosstalk. Small box monitors are placed surrounding each dipole source to receive the dipole power.

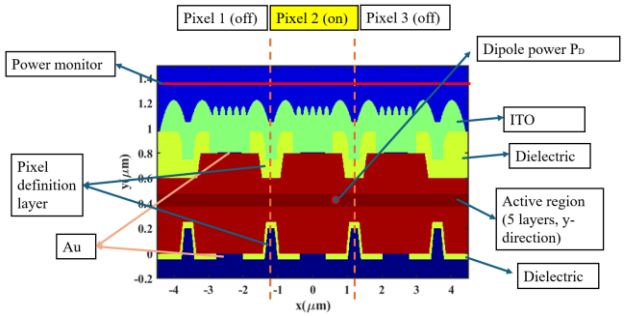

Figure 2. Schematic of FDTD CMQW microLED simulation model.

To precisely calculate the optical response, we applied dipole cloud in the simulation model at x-y plane. In vertical y-direction, a total of 5 dipoles are simulated for 5 pairs of QW. In horizontal x-direction, a total of 25 dipoles are included and each dipole are spaced 50nm. For zincblende crystal structure, the dipoles oscillate equally along all the directions. Therefore, dipoles oscillate along all the x-, y-, z- direction need to be considered. To avoid confusion with dipole position (x, y), we denote the dipole oscillation directions to be (X, Y, Z).

The LEE of each dipole can be calculated as the power ratio between the power monitor to the dipole box monitor [6]:

$$LEE_d(X,Y,Z,x,y) = \frac{\int\int_{-4.5\mu m}^{4.5\mu m} P_E(X,Y,Z,x,y,W,\lambda)S(\lambda)dWd\lambda}{\int P_D(X,Y,Z,x,y,\lambda)S(\lambda)d\lambda}, \quad (1)$$

where P_E and P_D is the power received by power monitor and dipole monitor, respectively. S(λ) is the emission spectrum.

However, due to optical crosstalk, light emit from adjacent pixels is considered as stray light. Therefore, we define LEE_d' to be the effective LEE where the light emits from the original pixel.

$$LEE_d'(X,Y,Z,x,y) = \frac{\int\int_{-1.2\mu m}^{1.2\mu m} P_E(X,Y,Z,x,y,\lambda)S(\lambda)dWd\lambda}{\int P_D(X,Y,Z,x,y,\lambda)S(\lambda)d\lambda}, \quad (2)$$

The position dependence can be eliminated by considering electrical weightage.

$$LEE'(X,Y,Z) = \frac{\sum_{y=1}^{5}\int_{-4.5\mu m}^{4.5\mu m} LEE_d'(X,Y,Z,x,y)E(x,y)dx}{\sum_{y=1}^{5}\int_{-4.5\mu m}^{4.5\mu m} E(x,y)dx}, \quad (3)$$

where E(x, y) is position dependent electrical excitation. The final LEE result is the average of dipoles oscillating in all directions. The LEE′ results for (X, Y, Z) dipoles are 9.07%, 0.64%, and 9.45%, respectively. The LEE ′ for Y-oscillating dipole is significantly lower than the other two dipoles because the emit power is the strongest along the x-direction. The overall LEE′ is 6.4%.

To calculate crosstalk of the CMQW structure, the electrical and optical weight of all the dipoles need to be considered. The crosstalk can be calculated as:

$$CT(X,Y,Z) = \frac{\int_{-1.2\mu m}^{1.2\mu m} P_E(X,Y,Z,x,y,W)LEE_d'(X,Y,Z,x,y)E(x,y)dW}{\int_{-4.5\mu m}^{4.5\mu m} P_E(X,Y,Z,x,y,W)LEE_d'(X,Y,Z,x,y)E(x,y)dW}, \quad (4)$$

Figure 3 shows that the total crosstalk in CMQW microLED is 19.5%, which agrees well with the measured data from [3]. The crosstalk for (X, Y, Z) dipoles is 23%, 53%, and 17%, respectively. The crosstalk of y- oscillating dipoles are noticeably higher than the other two. However, due to the low LEE for Y-oscillating dipoles, it does not have a significant impact on the total result.

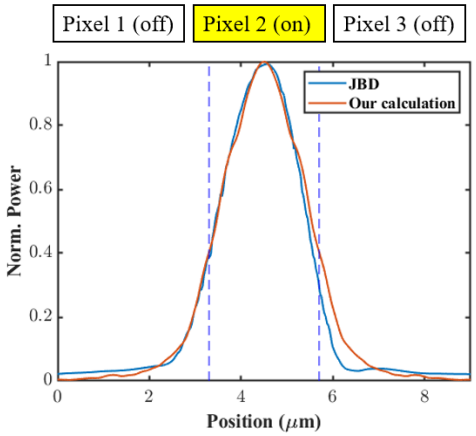

Figure 3. Comparison between simulated crosstalk and the measured data from Ref. [3].

4. Optimization

Due to the CMQW structure, the μLED behaves like a waveguide. At the same time, due to the existence of pixel definition layer, the μLED also behaves like a quasi-cavity. There are three ways to improve the EQE in such structure as indicated in Fig. 4(a). The first method is to modify the position of the CMQW to improve the constructive interference in the waveguide to increase the air mode and reduce the waveguide mode. However, the geometrical freedom in thin film CMQW structure is limited because the pixel definition pillar needs to be placed far from the

active layer, especially when the CMQW thickness is 100nm. By sweeping the p-AlGaInP thickness from 350nm to 500nm with a 10-nm step, the LEE of 5 pairs MQW only slightly fluctuates between 6.2% and 6.5%. The second method is to redirect the waveguide mode by optimizing the pixel definition layer as shown in Fig. 4(b). For bottom Si_3N_4 coated metallic layer, the height of the layer (H_B) is fixed at 200nm, while the tilt angle is modulated by the length (L_B). Similarly, for top dielectric pixel definition layer, the tilt angle is controlled by L_T.

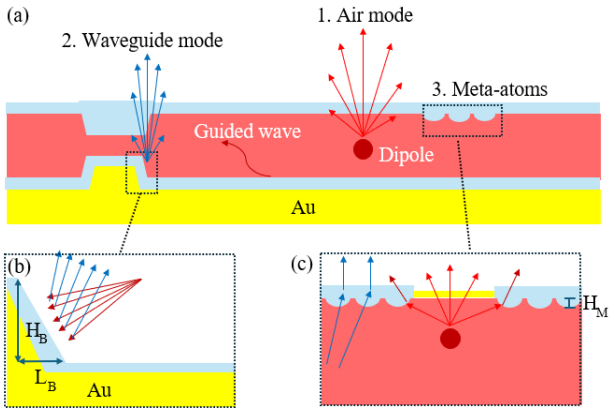

Figure 4. (a) Optical modes in CMQW structure. (b) Redirect guided wave by modifying pixel definition layer. (c) Meta-atoms on AlGaInP top surface improves light extraction for both air mode and redirected waveguide mode. Red arrow: emission from dipole sources. Blue arrow: redirected guided light.

Figure 5 indicates the optimization by sweeping L_T and L_B both from 0μm to 0.4μm. Limited by computer memory, we only considered dipoles placed in center of each pixel. On vertical direction, 5 dipoles are considered to average interference. Black dot indicates that LEE′=6.18% before optimization when L_T =0.1μm and L_B=0.14μm. By increasing L_T = 0.25 and L_B=0.4, LEE′ increases to 6.89%, corresponding to an 11% improvement.

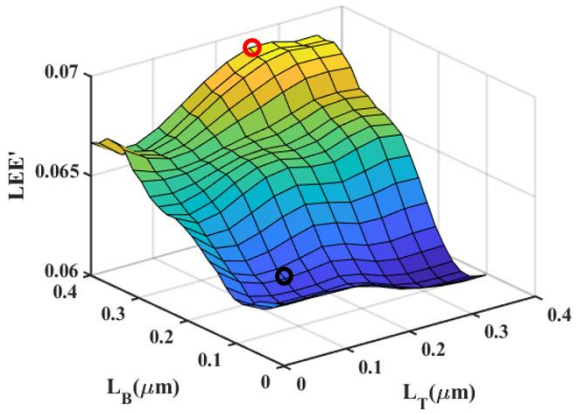

Figure 5. Colormap of LEE′ as a function of L_T and L_B.

The improvement by modulating the pixel definition layer is limited because most of light is still trapped in the structure due to the large refractive index differences between AlGaInP and Si_3N_4. To improve the light extraction, we consider the third method which incorporates meta-atoms at the interfaces between AlGaInP and Si_3N_4 as shown in Fig. 4(c). Due to the existence of the thin metallic electrode, the center of the pixel Among different meta-atoms, Moth-eye-like anti-reflection film is capable to increase light transmittance without inducing electrical conductivity issues. In our optimization, we fix the periodicity of the moth-eye structure to be 150nm and the diameter (D_M) to be 150nm. Figure 6 depicts the sweeping results by increasing the moth-eye structure depth H_M from 0 to 75nm. The LEE′ further increases from 6.89% to 8.17%, corresponding to another 18.6% improvement. By combining both methods, the LEE′ of the 5-layer center dipoles increases from 6.18% to 8.17%, corresponding to a total improvement of 32.2%.

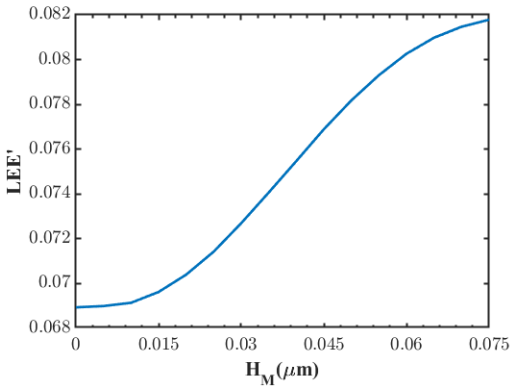

Figure 6. Simulated LEE′ as a function of moth-eye structure depth (H_M)

Based on the optimized geometrical values, dipole cloud is simulated for the optimized CMQW microLED. The LEE′ of the dipole cloud increases from 6.4% to 8.28%, which is improved by ~30%. We notice that the improvement for dipole cloud is slightly lower than the center dipoles because the redirection of pixel definition layer is optimized for center dipoles instead of edge dipoles. However, the total crosstalk only slightly improves from 19.5% to 15% with a narrower line shape.

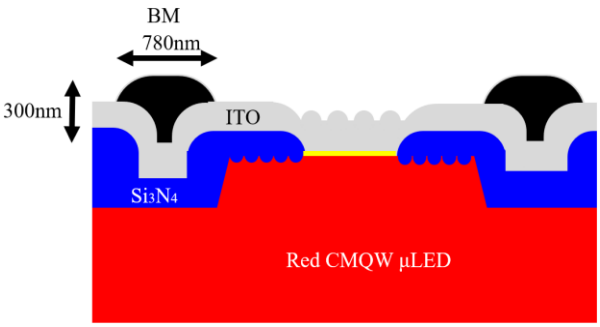

Figure 7. Schematic of red CMQW μLED with BM on top of the pixel definition layer.

As shown in Fig. 7, the optical crosstalk can be suppressed by implementing black matrix on the pixel definition layer. Such Carbon BM structure can be fabricated by both inkjet printing and photolithography. We have considered the dispersion of Carbon black and its refractive index is 1.8+0.7i at wavelength of 620nm. After applying BM, the total crosstalk dramatically decreases from 15% to 3.8%. Compared to unoptimized case (19.5%), the total crosstalk is suppressed by ×5. Due to the existence of black

matrix, the LEE decreases to 6.87%, which is still better than unoptimized case which is 6.4%. For a higher absorptive material such as Ta-doped black matrix, the total crosstalk can be further reduced to 2.8%, while the cost increases.

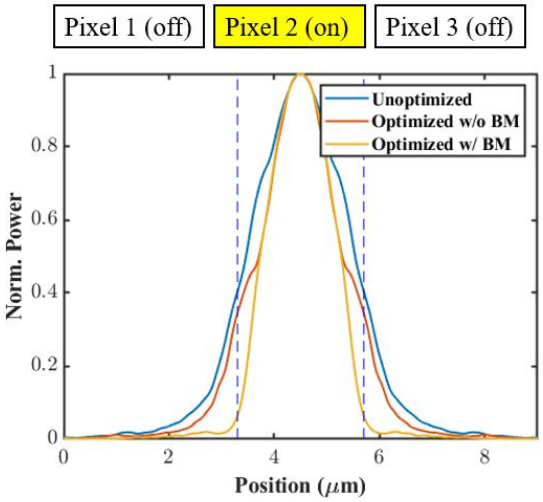

Figure 8. Comparison of simulated crosstalk between unoptimized and optimized CMQW microLED w/o and w/ BM.

5. Image quality

Figure 9 demonstrates the improvement in image quality achieved by incorporating the carbon BM. As shown in Figure 9(a), a high crosstalk level of 19.5% introduces noticeable image blur, particularly in regions containing sufficient details. By reducing the crosstalk to 3.8%, the image quality is significantly enhanced (Fig. 9(b)). This improvement is reflected in the multi-scale structural similarity index (MS-SSIM), which increases from 0.978 to 0.987 after optimization, indicating a closer match to the original image.

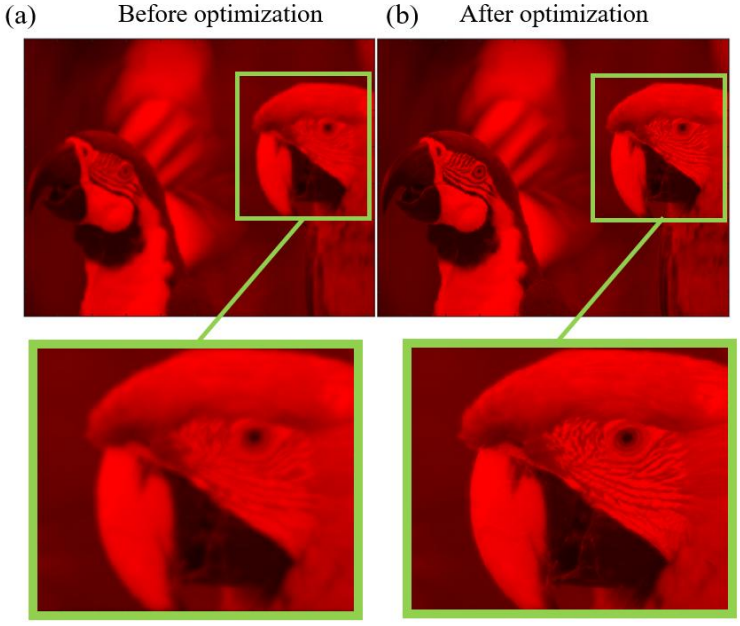

Figure 9. Simulated image of CMQW red μLED (a) before and (b) after optimization.

6. Conclusion

We have successfully optimized continuous multiple-quantum-well (CMQW) red AlGaInP microLEDs by modifying the pixel definition layer and implementing moth-eye meta-atoms. These optimizations have increased the light extraction efficiency (LEE) from 6.4% to 8.28%, representing an improvement of ~30%. Additionally, the overall crosstalk between adjacent pixels has been reduced from 19.5% to 15%. By implementing BM, the crosstalk dramatically decreases to 3.8%, while it still maintains a high LEE of 6.87%. This significant reduction in crosstalk enhances overall image quality and minimizes image blur. Further enhancements can be achieved by controlling current diffusion and further optimizing the meta-atom structures. The development of these high-efficiency low-crosstalk red AlGaInP microLEDs can significantly reduce the power consumption and improve image quality of augmented reality (AR) eyeglasses, advancing their potential to be integrated with daily life.

7. References

1. Lin C.-C., Wu Y.-R., Kuo H.-C. et al. The Micro-LED Roadmap: Status Quo and Prospects. Journal of Physics: Photonics. 2023;5(4):042502.
2. Huang Y., Hsiang E.-L., Deng M.-Y. et al.. Mini-LED, Micro-LED and OLED displays: Present status and future perspectives. Light: Science & Applications. 2020;9(1):105.
3. Li Q., Tan W., Zhu Y. et al. 11-1: Invited Paper: MicroLED Displays for Augmented Reality Smart Glasses. SID Symposium Digest of Technical Papers; 2024;55(1):104-107 Wiley Online Library.
4. Bauch M., Theodoros D. Design of ultrathin metal-based transparent electrodes including the impact of interface roughness. Materials & Design. 2016;104:37-42.
5. Gou F., Hsiang E.-L., Tan G. et al. Angular color shift of micro-LED displays. Optics Express. 2019;27(12):A746-A757.
6. Qian, Y., Yang, Z., Huang, Y. et al. Directional high-efficiency nanowire LEDs with reduced angular color shift for AR and VR displays. Opto-Electronic Science. 2022;1(12), 220021.